Sensitivity of channel profiles to precipitation properties in mountain ranges

Shiliang Wu,[1] Rafael L. Bras,[2] and Ana P. Barros[3]

Received 1 May 2004; revised 3 October 2005; accepted 20 December 2005; published 28 March 2006.

[1] The stream power erosion law, which describes the erosion rate as a function of channel discharge and gradient, has often been used for modeling landscape evolution in regions dominated by fluvial processes. However, most previous studies utilizing the stream power erosion law simply use drainage area as a surrogate for channel discharge. Despite its convenience this simplification has important shortcomings. Specifically, it ignores the effects of precipitation properties on channel discharge and hence erosion rate, and it ignores the interactions between mountain ranges and precipitation properties. By using the stream power erosion law together with the geomorphoclimatic instantaneous unit hydrograph we provide a method for linking the landscape evolution and precipitation properties directly. Our results demonstrate that the channel profile is sensitive not only to the total precipitation but also to precipitation properties like the rainfall frequency, intensity, duration, and their distribution in space. The channel profile is most sensitive to the variation of rainfall intensity and less sensitive to rainfall frequency and duration. Shorter and more intense rainfall could lead to significantly higher erosion rate and flatter channel profiles compared to longer and less intense rainfall. The spatial variation of precipitation can also influence the evolution of channel profile. Even if the total precipitation remains spatially homogeneous, different spatial behavior of rainfall intensity and rainfall duration may lead to different steady state river profiles. The channel profile tends to be flatter under the conditions of increasing rainfall intensity and decreasing rainfall duration with elevation and vice versa.

Citation: Wu, S., R. L. Bras, and A. P. Barros (2006), Sensitivity of channel profiles to precipitation properties in mountain ranges, *J. Geophys. Res.*, *111*, F01024, doi:10.1029/2004JF000164.

1. Introduction

[2] The evolution of topography is dictated by tectonic forcing and climate-driven erosion [e.g., *Snyder et al.*, 2000; *Whipple*, 2004], and steady state channel profiles are the result of the balance between erosion processes and tectonic uplift [e.g., *Willgoose and Bras*, 1991; *Montgomery*, 1994; *Burbank et al.*, 1996; *Tucker and Bras*, 1998, 2000; *Whipple and Tucker*, 1999, 2002; *Roe et al.*, 2002, 2003]. The ability of a river to erode bedrock and remove sediments is mainly dependent on the channel's discharge and slope, whereas the channel's discharge is closely associated with the volume and space-time patterns of precipitation in upstream drainage areas. It is thus reasonable to expect that precipitation properties play an important role in determining erosion rates, and consequently river channel profiles. Mountain ranges exert large control on regional weather and on the spatial and temporal variations of precipitation, and strong orographically driven altitudinal gradients in precipitation are a basic feature of mountain climates [e.g., *Barros and Lettenmaier*, 1994; *Barros et al.*, 2000]. Hence there is a potential for strong interaction between the evolution of channel profiles in mountain ranges and precipitation characteristics [*Barros et al.*, 2006]. *Masek et al.* [1994] proposed that orographic precipitation and high erosion rates are responsible for the steep frontal slope and high peaks of the Beni region in Andes and the Himalayan front. *Molnar* [2001] suggested that a change in climate toward more arid conditions in the late Cenozoic leads to increased erosion rates despite decreases in precipitation and discharge. His explanation is an increase of the frequency of large floods.

[3] In order to investigate the effects of precipitation on landscape evolution, it is necessary to model the erosion rate, which is often described as a function of channel discharge and local gradient as in the well-known "stream power erosion law" [e.g., *Whipple and Tucker*, 1999; *Whipple et al.*, 1999; *Lave and Avouac*, 2001]. Because of its simplicity and apparent mechanistic basis, the stream power erosion law has often been used for modeling river incision into bedrock in a fluvial system [e.g., *Howard and Kerby*, 1983; *Seidl and Dietrich*, 1992; *Rosenbloom and Anderson*, 1994; *Howard et al.*, 1994; *Hancock et al.*, 1998; *Sklar and Dietrich*, 1998; *Stock and Montgomery*, 1999; *Whipple et*

[1]Division of Engineering and Applied Sciences, Harvard University, Cambridge, Massachusetts, USA.
[2]Department of Civil and Environmental Engineering, Massachusetts Institute of Technology, Cambridge, Massachusetts, USA.
[3]Department of Civil and Environmental Engineering, Duke University, Durham, North Carolina, USA.

0148-0227/06/2004JF000164$09.00

al., 2000a; *Tucker and Whipple*, 2002]. However, most of the previous applications of the stream power erosion law have used drainage area as a proxy for water discharge. Assuming that discharge is proportional to drainage area to some power introduces a strong functional constraint on the precipitation properties. For example, this precludes the possibility of an interaction between landform and topography and the atmosphere, and therefore storms and precipitation [*Roe et al.*, 2002, 2003]. It also precludes the possibility of linking erosion rate with detailed precipitation patterns and properties [*Barros et al.*, 2004, 2006].

[4] *Tucker and Bras* [2000] developed a stochastic approach to model the role of rainfall variability in drainage basin evolution and found that rainfall variability can have an impact equal or greater than that of mean rainfall amount under some circumstances. Several basic assumptions in their work apply only to small basins: (1) Each storm can be approximated as a steady and spatially uniform rainfall throughout its duration; (2) at each point in the landscape, runoff (if nonzero) produces a constant, steady discharge equal to the runoff rate times the contributing area; (3) flood duration is equal to storm duration. The first geomorphological model using a realistic hydrograph was presented by *Solyom and Tucker* [2004]. By assuming self-similar hydrograph shapes, they described the peak flow as a simple function of runoff rate, storm duration and basin length. According to their simulation results, this assumption is acceptable when the storm duration number (defined as the ratio of storm duration over the time of concentration of the catchment) is less than 0.5 which implies that their approach is ideal for large catchments and/or storms of short duration only. The time of concentration is the time that it takes for a drop of water to travel from the farthest point in the catchment divide to the outlet.

[5] The geomorphoclimatic instantaneous unit hydrograph (GCIUH), first introduced by *Rodriguez-Iturbe et al.* [1982] and based on the geomorphologic instantaneous unit hydrograph (GIUH) of *Rodriguez-Iturbe and Valdes* [1979], implies a rainfall-runoff relationship that is theoretically only dependent on geomorphologic and climatic data. By incorporating the stream power erosion law and the GCIUH we are able to investigate the interaction between channel profiles and specific precipitation characteristics, particularly as they change over mountainous terrain. Rainfall characteristics that are studied here include frequency, intensity and duration as well as the probability distribution functions (PDFs) of rainfall intensity and duration. We also discuss the sensitivity of the results to variation in the parameters of the stream power erosion law.

2. Theory

2.1. Stream Power Erosion Law and the GCIUH

[6] The general form of the stream power erosion model represents the erosion rate, E, as a power law function of water discharge, Q and local channel gradient, S:

$$E = KQ^m S^n \tag{1a}$$

where the discharge exponent m and area exponent n are positive constants with values that depend on erosion processes, basin hydrology, and channel hydraulic geometry [*Whipple et al.*, 1999]; K is the erosion coefficient with dimension that depends on the discharge exponent m.

[7] The stream power erosion model has been widely used, and in most previous research, equation (1a) was reformulated into the following form (Table 1 summarizes some of those past uses and values of parameters that appear in the literature):

$$E = K' A^{m'} S^{n'} \tag{1b}$$

where the upstream drainage area A serves as a surrogate for the variable of discharge Q in (1a) and K' is the corresponding erosion coefficient. The underlying assumption is that the discharge can be approximated well by a power function of the drainage area:

$$Q = k_1 A^c \tag{2}$$

where K_1 and c are constants. However, this assumption implies a strong functional constraint on the precipitation distribution, and precludes the possibility of an interaction between orography and precipitation [*Roe et al.*, 2002, 2003]. In addition, it precludes the possibility of linking erosion rate with detailed precipitation patterns and properties.

[8] Following the work of *Henderson* [1963] and *Rodriguez-Iturbe et al.* [1982], *Bras* [1990] derived the peak discharge Q_p (in m^3/s) of the channel flow as follows

$$Q_p = 2.42 \frac{i_r t_r A}{\prod_i^{0.4}} \left(1 - \frac{0.218 t_r}{\prod_i^{0.4}}\right) \qquad t_r \le t_b \tag{3a}$$

$$Q_p = 2.778\ i_r A \qquad t_r \ge t_b \tag{3b}$$

where i_r is the effective rainfall intensity (in cm/hr), $t_r$is the rainfall duration (in hours), A is the upstream drainage area (in km^2), t_b is the concentration time of the catchment, which depends on basin geomorphology and channel hydraulic properties

$$\prod_i = \frac{x^{2.5}}{i_r A R_L \alpha^{1.5}} \tag{4}$$

$$\alpha = \frac{S^{1/2}}{n^* b^{2/3}} \tag{5}$$

$$t_b = \frac{\prod_i^{0.4}}{0.436} \tag{6}$$

where x is the along channel distance (in km) with $x = 0$ defined as the drainage divide; R_L is a constant reflecting the law of stream lengths with a typical range between 1.5 and 3.5; n^* is the Manning roughness coefficient; and b is the width of the stream (in m).

[9] The use of "effective rainfall intensity" in the above formulation ignores the impact that variable infiltration will have on the production of runoff. Implicitly we are assuming that infiltration is a constant that has been eliminated

Table 1. Selected Literature With Applications of the Stream Power Erosion Law

Reference	Form of the Stream Power Erosion Law	Values Used or Reported for m & n	Notes/Assumptions
Howard and Kerby [1983]	$E = KA^mS^n$	m = 0.44; n = 0.68	The values for m and n are derived from field data for bedrock channels measured in Virginia; the model predicted values are m = 0.38 and n = 0.81.
Howard et al. [1994]	$E = KA^mS^n$	m ≈ 0.25; n = 0.7	The bedrock erosion is proportional to bed shear stress; most erosion occurs as a result of high (flood) discharges.
Seidl et al. [1994]	$E = KA^mS^n$	m/n = 1	The river incision rate into bedrock is proportional to the stream power and the peak runoff events scaled with drainage area.
Montgomery [1994]	$E = KA^mS^n$	m = 1; n = 1	Erosion is proportional to stream power (the product of water discharge and local valley slope).
Rosenbloom and Anderson [1994]	$E = KA^mS^n$	m = 1; n = 1	
Moglen and Bras [1995]	$E = KA^mS^n$	m = 1; n = 2	Assumes the erosion is "detachment-limited".
Hancock et al. [1998]	$E = KA^mS^n$	various	m = 0.2∼0.3 and n = 2/3 for a shear stress rule; m = 0.3∼0.4 and n = 1 for a steam power rule.
Sklar and Dietrich [1998]	$E = KA^mS^n$	various	It is difficult to obtain unique values for K, m and n due to reasons such as there is very little data exist to either support or calibrate the stream power law.
Stock and Montgomery [1999]	$E = KA^mS^n$	various	m = 0.3∼0.5, n = 1 for rivers with stable base levels; m = 0.1∼0.2 for rivers with base levels that lower rapidly enough to create knickpoints.
Whipple and Tucker [1999]	$E = KA^mS^n$	m/n = 0.5; n = 1∼2	The m/n ratio is in a range of 0.35∼0.6.
Tucker and Bras [2000]	$E = KQ^mS^n$	various	m ≈ 0.5 and n ≈ 1 if erosion rate is proportional to excess shear stress; m ≈ 0.3 and n ≈ 0.7 if erosion rate depends on unit stream power.
Whipple et al. [2000a]	$E = KA^mS^n$	various; m/n = 0.35∼0.6	n = 2/3∼1 for erosion by plucking; n = 5/3 for erosion by suspended-load abrasion.
Whipple et al. [2000b]	$E = KA^mS^n$	m = 0.4; n = 1	Field data from the Ukak River Site best fit to $n = 0.4 \pm 0.2$.
Snyder et al. [2002]	$E = KA^mS^n$	m = 0.5; n = 1	
Roe et al. [2003]	$E = KQ^mS^n$	m = 1/3; n = 2/3	If the erosion rate depends on the stream power, m/n = 1.0; if it depends on the basal shear stress or the unit stream power, m/n = 0.5.
Solyom and Tucker [2004]	$E = KA^mS^n$		For large basins or short storms with m systematically smaller than that in smaller basins.

before the distributions of rainfall characteristics are computed. It would be possible to include variable infiltration in our analysis, but the reality is that the assumptions of the stochastic model of precipitation, and in particular the assumption of constant storm intensity, are probably far more significant. Including infiltration controls in addition to the stochastic representation of precipitation will add degrees of freedom to the model and make the interpretation of model results more difficult and not necessarily better given the first-order assumptions already made. We believe that these approximations are compatible with the research goals of this study and will yield correct behavior over the long-term averages that we are computing.

[10] We represent the channel width b using the empirical hydraulic geometry relationships [*Leopold and Maddock*, 1953; *Tucker and Bras*, 2000; *Snyder et al.*, 2000; *Tucker*, 2004] that relate the channel width at a given cross section to a characteristic flow, here assumed to be that corresponding to the total mean annual discharge:

$$b = K_b\bar{Q}^d = K_b\left(K_f\bar{i}_r\bar{t}_rA\right)^d \tag{7}$$

where $\bar{Q}$ is the annual mean channel discharge, d is a constant exponent, K_b is a dimensional coefficient (units and value used for the numerical experiments in this work are given in Table 2. The choice of parameter K_b was such that the channel width at the basin outlet was about 100–300m, depending on the total annual mean channel discharge.), K_f is the frequency of rainfall, $\bar{i}_r$ and $\bar{t}_r$ are the mean effective rainfall intensity and duration, respectively. Note that as implied by equation (7), b increases with the upstream area A since the annual total mean discharge increases with the contributing area. *Montgomery and Dietrich* [1992] proposed a very simple relationship between the distance from the divide, x, and its upstream drainage area A given by

$$A = \frac{1}{3}x^2 \tag{8}$$

The exponent d in this context should correspond to the geometric variation of width along a stream. *Leopold and Maddock* [1953] defined this variation for flow of the same recurrence. The use of the total mean discharge in Equation (7) does not necessarily guarantee that condition. Nevertheless this paper uses a value of $d = 0.5$, the value empirically obtained for the "along the river" variation by *Leopold and Maddock* [1953].

[11] The rainfall-runoff relationship implied by equations (3a) and (3b) does not require calibration of empirical parameters, and provides a simplified direct link between climate and catchment geomorphology [*Bras*, 1990]. Figure 1 illustrates the dependence of Q_p on i_r and t_r at a given channel location in an idealized basin and it shows that variations in rainfall intensity and duration have different

Table 2. Values/Ranges of Parameters Used in the Numerical Simulation

Parameter	Value/Range	Units	Notation/Notes
U	2	mm/year	rock uplift rate
E	—	mm/year	erosion rate
m	1/3	—	discharge exponent in the stream power erosion law
n	2/3	—	area exponent in the stream power erosion law
K	4×10^{-11}	$m^{(1-3m)}s^{(1-m)}$	erosion coefficient in the stream power erosion law; unit depends on m (e.g., [K] = $s^{-2/3}$ for m = 1/3)
d	0.5	—	exponent in the channel width–discharge relationship
K_f	15–100 (default: 50)	$year^{-1}$	frequency of rainfall
$\bar{i}_r$	5–40 (default: 20)	mm/hr	mean rainfall intensity
$\bar{t}_r$	0.5–4 (default: 2)	hours	mean rainfall duration
$f(i_r)$	—	—	probability distribution of rainfall intensity
$f(t_r)$	—	—	probability distribution of rainfall duration
p	—	mm/year	annual precipitation amount; $p = K_f \bar{i}_r \bar{t}_r$
R_L	3	—	coefficient in the stream length law
b	—	m	width of the stream
K_b	0.01	$m^{-1/2}yr^{1/2}$	coefficient in the hydraulic geometry relation
n*	0.05	—	manning roughness coefficient
x_c	1.5	km	location of the channel head from the drainage divide
L	30	km	maximum channel length
A	—	km^2	upstream drainage area
Q_p	—	m^3/s	channel peak discharge

implications for rainfall-runoff response, and consequently peak discharge.

[12] By assuming a simple triangular hydrograph as shown in Figure 2, the channel discharge Q at time t can be written as

$$Q(t) = Q_p \frac{t}{t_p} \qquad \text{when } t <= t_p \tag{9a}$$

$$Q(t) = Q_p \frac{t_r + t_b - t}{t_r + t_b - t_p} \qquad \text{when } t > t_p \tag{9b}$$

where t_p is the time to peak discharge:

$$t_p = 0.585 \prod_i^{0.4} + 0.75 t_r \tag{9c}$$

We assume that there is no overlap of hydrographs, therefore the long-term time-averaged value of erosion rate E (see equation (1a)) is

$$\bar{E} = KS^n K_f (\bar{t}_r + \bar{t}_b) \int_0^\infty \int_0^\infty \int_0^{t_r+t_b} Q(t)^m / (t_r + t_b) f(i_r) f(t_r) \cdot dt di_r dt_r \tag{10}$$

where $f(i_r)$ and $f(t_r)$ are the probability distribution functions (PDFs) of i_r and t_r, respectively. The triple integration in equation (10) is over all possible storm intensities i_r and durations t_r and over the resulting random duration of the hydrograph. It is assumed that the sediment transport is coincident with the hydrograph. The terms multiplying the integrals convert the result to a mean annual erosion value. Note that the mean time of concentration, $\bar{t}_b$, results from the integration of equation (6) over the probability distribution of rainfall intensities. It is also a function of downstream distance, x. We assume that i_r and t_r are independent random variables. We recognize that this is not the case in reality, but it is a commonly made assumption when the interest lies in very long average behavior. Usually $f(i_r)$ and $f(t_r)$ can be closely approximated by exponential distributions [e.g., *Bacchi et al.*, 1994; *Goel et al.*, 2000; *Tucker and Bras*, 2000]:

$$f(i_r) = \frac{1}{\bar{i}_r} \exp\left(-\frac{i_r}{\bar{i}_r}\right) \tag{11}$$

$$f(t_r) = \frac{1}{\bar{t}_r} \exp\left(-\frac{t_r}{\bar{t}_r}\right) \tag{12}$$

We utilize these exponential approximations as the default PDFs of i_r and t_r in this study. As will be discussed later, we also use the uniform distributions for i_r and t_r in investigating the sensitivity of channel profiles to different PDFs of i_r and t_r (refer to Figures 3a and 3b for the shapes of PDFs for i_r and t_r).

[13] Because the regions we are concerned with here are small relative to geologic spatial scales, we can assume that the uplift rate (or base level lowering rate) U is spatially constant [*Moglen and Bras*, 1995]. Under steady state conditions we have:

$$\bar{E} = U \tag{13}$$

From equations (3)–(9), we know that Q, Q_p, Π_i, α, t_b and b are all dependent on the downstream distance x and local channel gradient S. For notational convenience, we write the integration term in equation (10) as

$$X = K_f (\bar{t}_r + \bar{t}_b) \int_0^\infty \int_0^\infty \int_0^{t_r+t_b} Q(t)^m / (t_r + t_b) f(i_r) f(t_r) dt di_r dt_r \tag{14}$$

With given PDFs of i_r and t_r, X is only dependent on x and S, that is, $X = X(x, S)$. Then using (10) and (14), we can rewrite equation (13) as

$$S = \frac{U^{1/n}}{K} X(x, S)^{-1/n} \tag{15}$$

[14] With known geomorphology properties of the drainage area (such as, R_L and n*) as well as the uplift

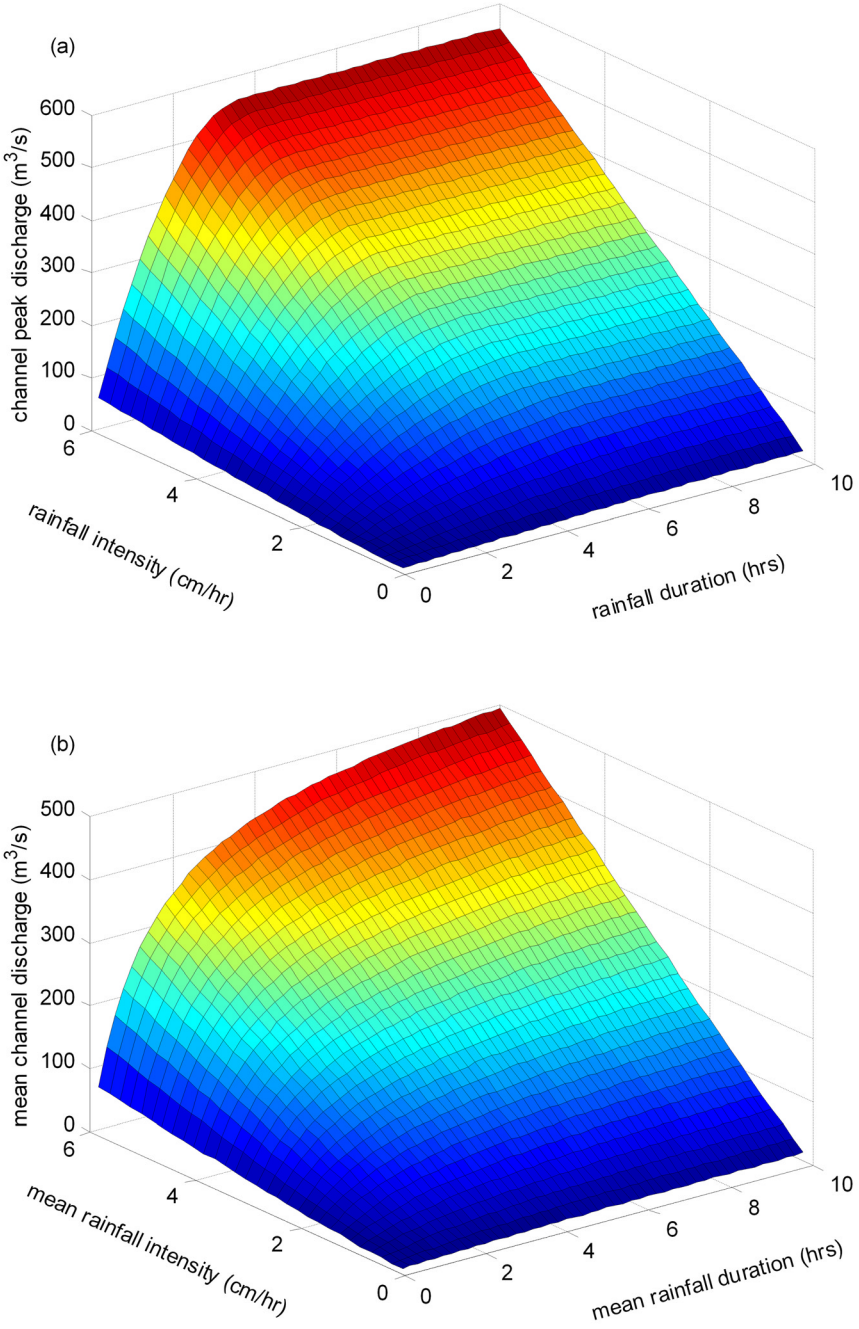

Figure 1. Effects of rainfall intensity and rainfall duration on channel peak discharge. (a) Channel peak discharge resulting from a single storm with different rainfall intensity and duration; (b) annually averaged channel peak discharge for different annual mean rainfall intensity and duration. Both plots are for station discharge (at location x = 10 km).

or base level lowering rate, U, we can describe the steady state channel gradient S as a function of x by solving equation (15). Furthermore, we can obtain the equilibrium channel profile $z = z(x)$ by recognizing that $S(x) = \partial z/\partial x$ where z is the channel bed elevation.

2.2. Numerical Implementation

[15] Because of the complex relation between X and S (Q_p is dependent on S as shown by equations (3)–(5)), equation (15) cannot be resolved analytically. Therefore we seek a numerical solution by using the iteration method described in detail below (For the numeric values and ranges of parameters used in the numerical simulation, refer to Table 2). Keep in mind that the solution of equation (15) is for channel profiles under steady state conditions.

[16] We apply the numerical experiment in the domain defined by $x_c < x < L$, where L is the maximum channel length and is taken to be 30 km [*Roe et al.*, 2003], x_c is the critical drainage length required for the formation of fluvial

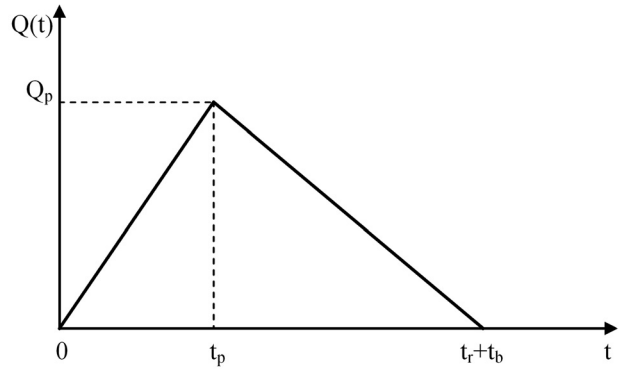

Figure 2. The triangular hydrograph with peak discharge of Q_p and the time to peak t_p; t_r is the duration of the storm, and t_b is the concentration time of the catchment.

channels and is set to 1.5 km (from this point up to the drainage divide where $x = 0$, other diffusive processes such as soil creep may dominate over fluvial processes). The base level is fixed at zero, that is at $x = L$, $z = 0$.

[17] The discrete grid is first set for the whole domain, and for any location x_i (i runs from 1 to n with $x_1 = L$ and $x_n = x_c$) we carry out the following steps.

[18] 1. Give a tentative value (for example, any value between 0.1 and 0.5) S_{old} for S and calculate X, as well as Q_p.

[19] 2. Calculate the new value for S_{new} from equation (15).

[20] 3. If the difference between S_{new} and S_{old} is less then 1% of S_{old}, then go to step (d); otherwise, replace S_{old} with S_{new} and repeat steps (b)$\sim$(c).

[21] 4. The steady state local channel gradient at location x_i is then $S_i = S_{new}$. Then calculate the elevation of channel at location x_i by $z_i = z_{i-1} + (x_{i-1} - x_i) * S_i$. A good initial "guess" for the tentative value of S_{old} is helpful in reducing the number of iterations and in increasing computational efficiency, thus a good candidate for S_{old} at location x_i is S_{i-1}.

3. Sensitivity Analysis

[22] The GCIUH tells us that the discharge of a drainage area with certain geomorphology is controlled by the characteristics of rainfall: rainfall intensity, rainfall duration and frequency. Figure 1a shows the channel peak discharge Q_p resulting from a single storm with different rainfall intensity i_r and duration t_r and Figure 1b shows the annually averaged channel peak discharge $\bar{Q}_p$ for different annual mean rainfall intensity $\bar{i}_r$ and duration $\bar{t}_r$. From Figure 1a we can see that the channel peak discharge has different responses to variations of different precipitation characteristics. When the rainfall duration t_r is smaller than t_b (the base time of the IUH), the peak discharge Q_p increases quickly with the increase of t_r; when t_r is larger than t_b, the variation of t_r has no influence on Q_p. On the other hand, Q_p always increases proportionally with the increase of rainfall intensity i_r. Figure 1b illustrates the similar feature: $\bar{Q}_p$ becomes less and less sensitive to the variation of $\bar{t}_r$ with the increase of $\bar{t}_r$ while it is always very sensitive to the variation of $\bar{i}_r$. This implies that with the same annual precipitation, different precipitation patterns can result in different channel discharges. The stream power erosion law suggests that the channel discharge plays a critical role in determining the erosion rate and hence the evolution of channel profiles. So we expect that the equilibrium channel profile is sensitive to specific rainfall characteristics as discussed in detail below.

3.1. Precipitation Parameters

[23] As the annual precipitation rate is a key factor in deciding the channel's discharge and hence the erosion rate, many investigators studying the impacts of precipitation on landscape evolution have focused on annual precipitation as the key precipitation descriptor [e.g., *Roe et al.*, 2002, 2003]. The mean annual precipitation p of a region is determined by

$$p = K_f \bar{i}_r \bar{t}_r \tag{16}$$

where K_f is the frequency of rainfall, $\bar{i}_r$ is the mean effective rainfall intensity and $\bar{t}_r$ mean rainfall duration. As shown in Figures 4a, 4b, and 4c, if any of the three parameters increases, implying a shift to a wetter climate, then the runoff and hence the stream power will also increase, resulting in a flatter channel and lower channel head.

[24] A more important feature, as we can see from Figure 4a, is that the steady state channel profile has different sensitivity to different precipitation properties. It is most sensitive to rainfall intensity and less sensitive to rainfall duration and frequency. This point is more obvious if we select the reference case with precipitation parameters

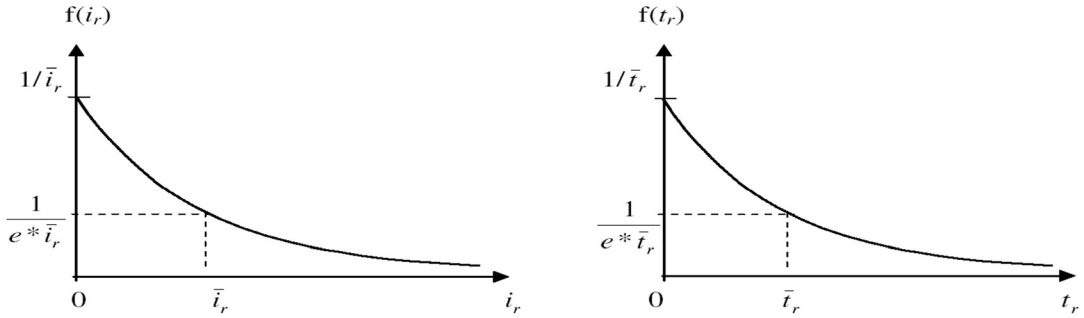

Figure 3a. PDFs of i_r and t_r with exponential distribution.

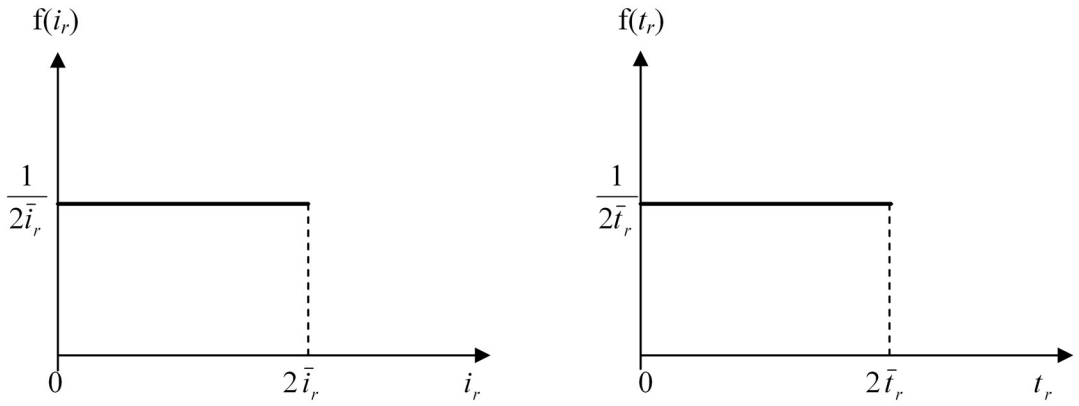

Figure 3b. PDFs of i_r and t_r with uniform distribution.

of K_f = 50/year, $\bar{i}_r$ = 20 mm/hour and $\bar{t}_r$ = 2 hours (under such conditions the elevation of the channel head is 2.1 km) and see how the steady state channel profile responds when the annual precipitation is decreased by 50% through the variation of $\bar{i}_r$, $\bar{t}_r$ and K_f respectively: if the mean effective rainfall intensity $\bar{i}_r$ decreases by 50% to 10 mm/hr, the channel head elevation will increase by 44% to 3.0 km; if the mean rainfall duration $\bar{t}_r$ decreases by 50% to 1 hr or the rainfall frequency K_f decreases by 50% to 25/year, the channel head elevation will increase by 29% to 2.7 km. It is worth emphasizing that the variations of the total annual precipitation are exactly the same for the sample cases discussed above, decreasing by 50% from 2000 mm/year to 1000 mm/year, but their effects on the steady state channel profiles are quite different with the resulting increase of channel head elevation ranging from 29 to 44%.

[25] Similarly, the steady state channel gradient is most sensitive to rainfall intensity and less sensitive to rainfall duration and frequency (Figure 4b). It can also be noticed from Figure 4b that while both the channel profile and slope change significantly with the variation of total precipitation amount, there is no significant effect on the concavity index θ. The concavity index θis here defined as the exponent in an empirical relationship $S = K_S A^{-\theta}$ [e.g., *Flint*, 1974; *Roe et al.*, 2002] where K_S is a dimensional coefficient. The relative area in Figure 4b is defined as the ratio of the

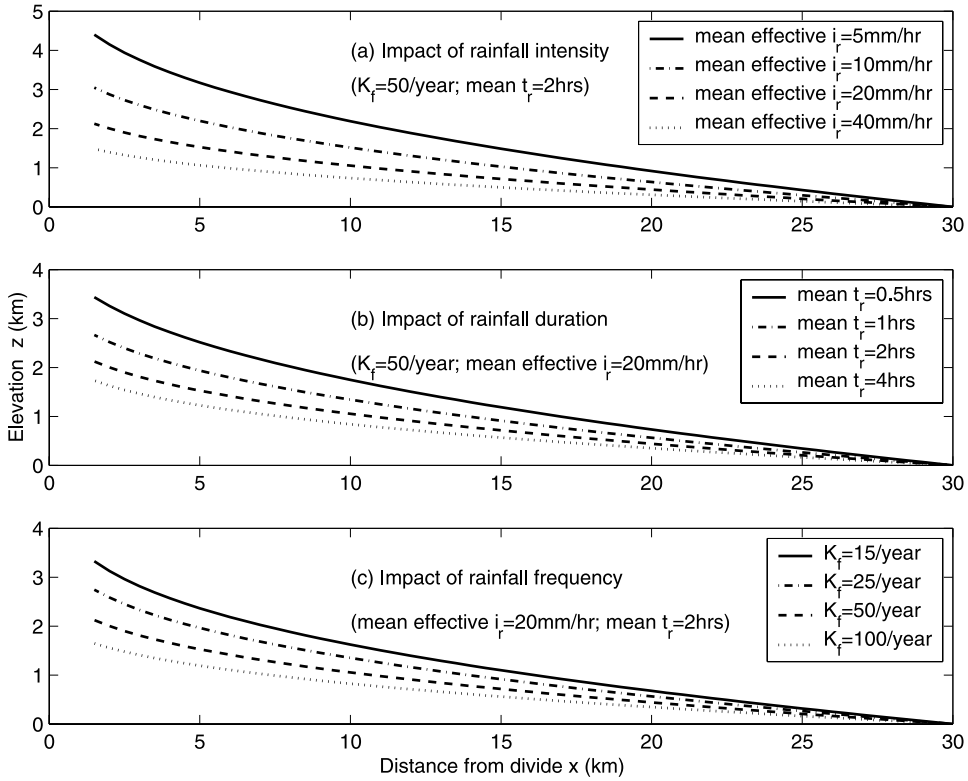

Figure 4a. Impact of (a) rainfall intensity, (b) rainfall duration, and (c) rainfall frequency on steady state channel profile.

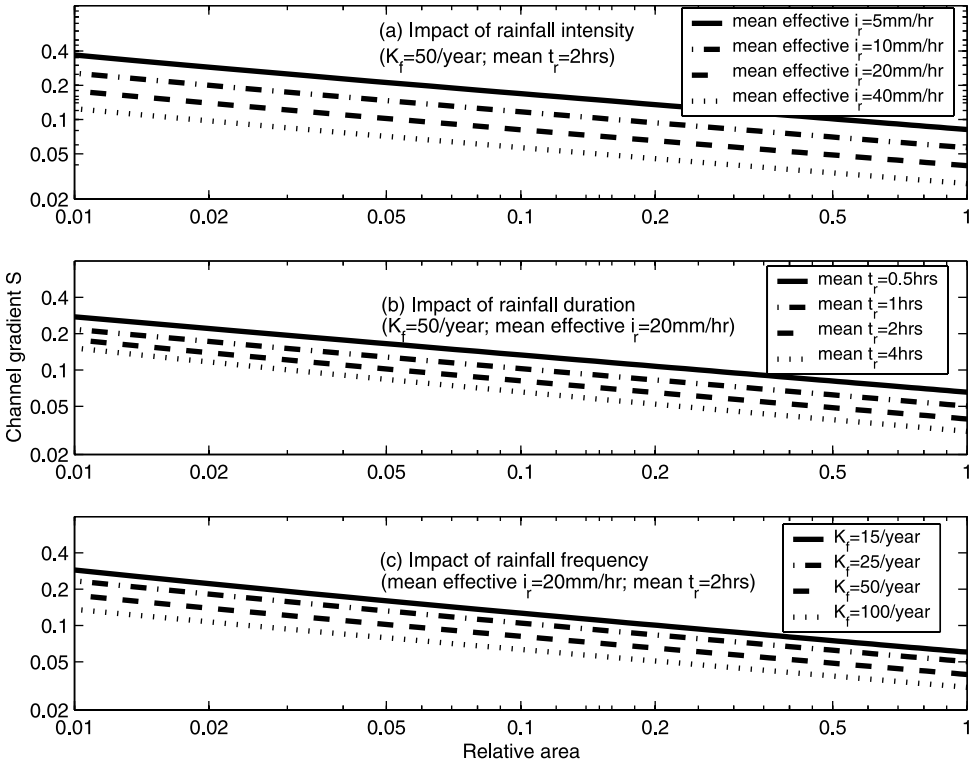

Figure 4b. Impact of (a) rainfall intensity, (b) rainfall duration, and (c) rainfall frequency on steady state channel slope; the relative area is defined as the ratio of the upstream drainage area to the total area of the whole basin.

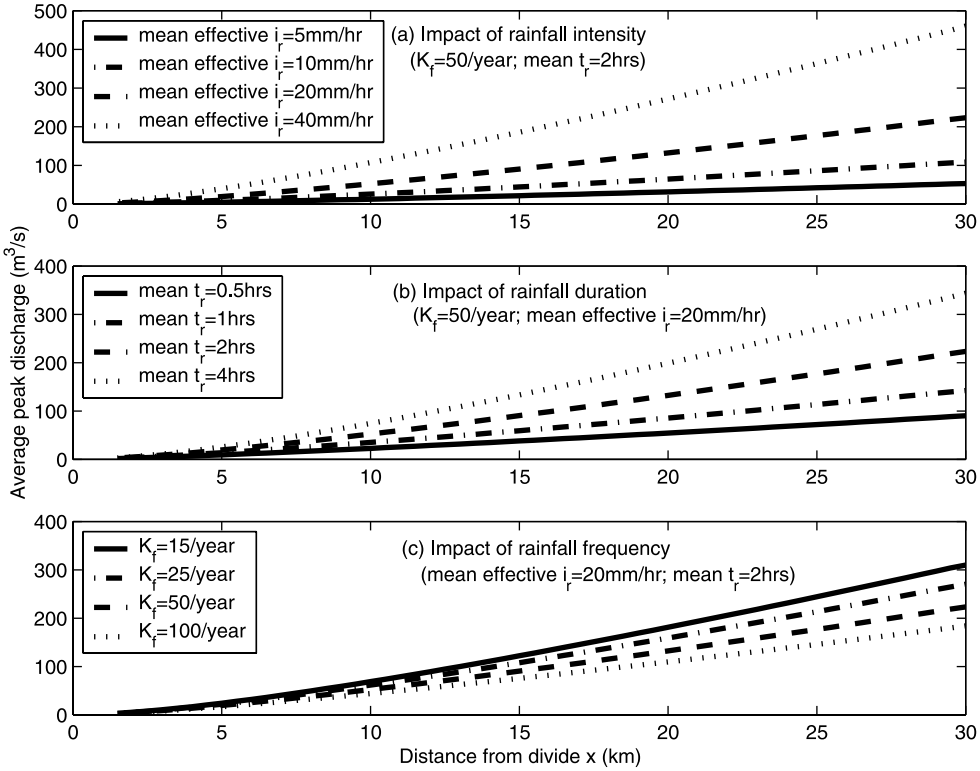

Figure 4c. Impact of (a) rainfall intensity, (b) rainfall duration, and (c) rainfall frequency on annual mean channel peak discharge.

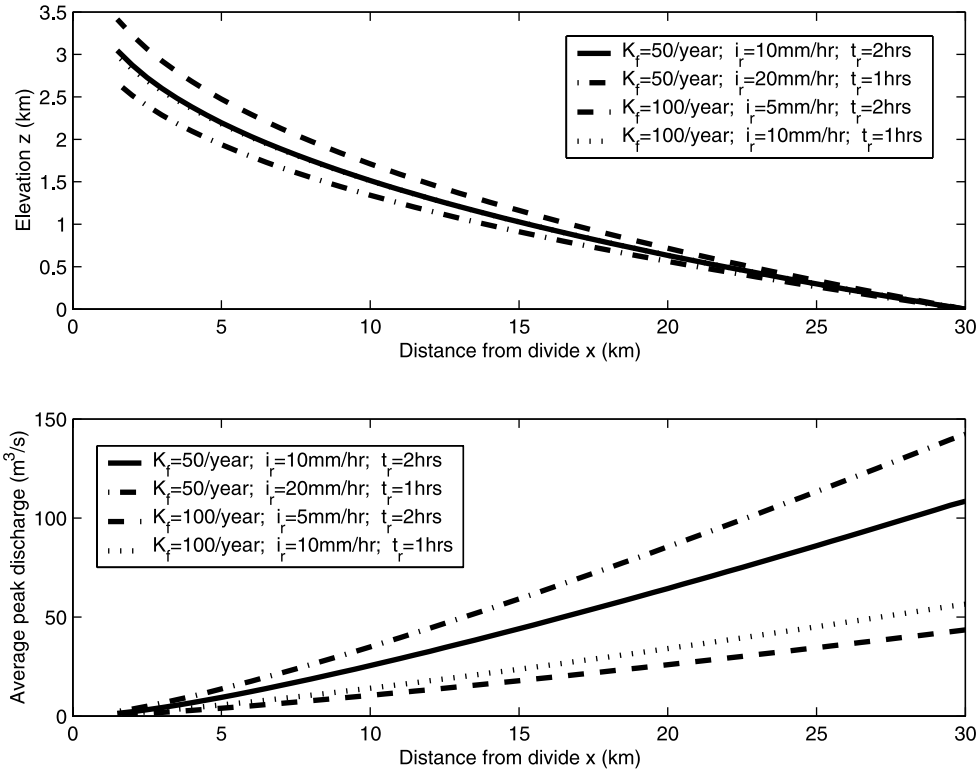

Figure 5a. Impact of precipitation properties on (top) steady state channel profile and (bottom) average peak discharge; both rainfall intensity i_r and rainfall duration t_r assume exponential probability distribution as shown in Figure 3a.

drainage area upstream of point x to the total area of the whole basin, and it is equal to x^2/L^2 according to Equation (8).

[26] The steady state channel profile's different sensitivities to $\bar{i}_r$, $\bar{t}_r$ and K_f arise from the different impacts of $\bar{i}_r$, $\bar{t}_r$ and K_f on the channel's peak discharge. As shown in Figure 4c, when the effective rainfall intensity decreases by 50%, the average peak discharge will always decrease by about 50%; but when the rainfall duration decreases by 50%, the peak discharge only decreases about 30–40%. As shown in Figure 1, the channel peak discharge at any location is always linearly proportional to the effective rainfall intensity, whereas the rainfall duration has the most influence on the (mean) peak discharge when it is shorter than the concentration time of the basin.

[27] To further investigate the importance of different precipitation parameters in controlling the channel profile, we conduct sensitivity analysis maintaining the annual total precipitation constant while varying the precipitation parameters $\bar{i}_r$, $\bar{t}_r$ and K_f. We find that if K_f is held fixed, and $\bar{i}_r$ increases while the product $\bar{i}_r$ and $\bar{t}_r$ is held fixed, therefore implying a shift of climate regime to shorter but more intense rainfall patterns, the profile of the channel becomes flatter and the channel head elevation decreases significantly (Figures 5a, top, and 5b, top). This can be explained by examining the channel peak discharge under these different conditions (Figures 5a, bottom, and 5b, bottom): for the same total precipitation, shorter and more intense rainfall would lead to higher channel peak discharge and hence higher erosion rate resulting in flatter channel profiles.

[28] Furthermore, Figures 5a and 5b illustrate that the channel profile and peak discharge are also sensitive to the probability distribution patterns of i_r and t_r. In Figure 5a, the PDFs for i_r and t_r are exponential distributions from equations (11) and (12) respectively (Figure 3a), while in Figure 5b, they are uniform distributions (Figure 3b):

$$f(i_r) = \frac{1}{2\bar{i}_r} \quad i_r \in (0, 2\bar{i}_r) \tag{17}$$

$$f(t_r) = \frac{1}{2\bar{t}_r} \quad t_r \in (0, 2\bar{t}_r) \tag{18}$$

[29] We can see, by comparing Figures 5a and 5b, that the use of the exponential distributions to describe $f(i_r)$ and $f(t_r)$ leads to steeper slopes and higher channel heads than the use of the uniform distribution. When i_r and t_r are assumed to be uniformly distributed, the channel head elevation decreases about 10∼15% compared to that under the condition of exponential distribution for a given $\bar{i}_r$ and $\bar{t}_r$. This can be explained by recognizing that the change of PDFs for i_r and t_r from the exponential to the uniform distribution implies more frequent rainfall events with higher intensity and longer duration. This is consistent with previous research results stating that the erosion rate is dominantly influenced by "extreme events", that is large

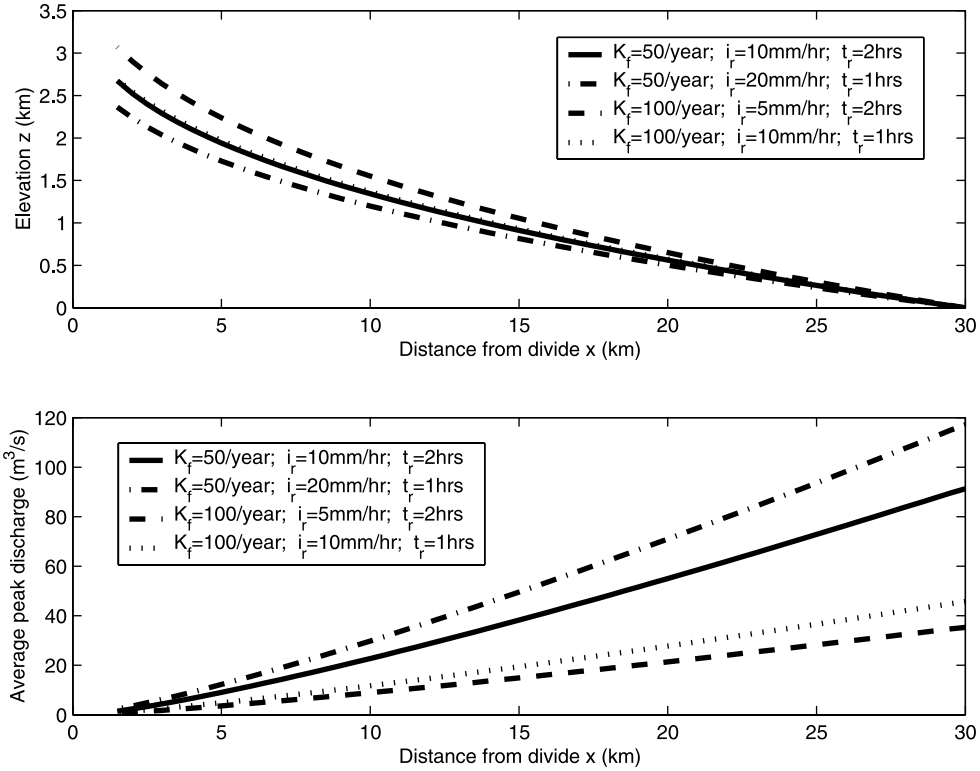

Figure 5b. Impact of precipitation properties on (top) steady state channel profile and (bottom) average peak discharge; both rainfall intensity i_r and rainfall duration t_r assume uniform probability distribution as shown in Figure 3b.

floods [e.g., *Wolman and Miller*, 1960; *Molnar*, 2001; *Montgomerey and Brandon*, 2002].

3.2. Spatial Patterns of Precipitation Parameters

[30] A fundamental feature of mountain climates is the presence of strong orographically driven gradients in precipitation [e.g., *Barros and Lettenmaier*, 1994]. There have been some studies on the interaction between orographic precipitation and landscape evolution [e.g., *Roe et al.*, 2003]. However, previously, the focus was only on precipitation amount and very little attention has been paid to the detailed precipitation properties. However, as seen in section 3.1, the steady state channel profile is not only sensitive to the total precipitation amount, but also to the storm characteristics. In order to study and compare the different sensitivities of the channel profile to specific precipitation characteristics, we need to keep the total precipitation amount constant in all the reference cases allowing us to separate the effects of different precipitation patterns from annual precipitation amounts.

[31] We study three simplified spatial precipitation patterns to demonstrate the effects of different orographic precipitation feedbacks on channel evolution. In all three cases, the frequency of rainfall is kept the same and the total precipitation also remains the same everywhere in the domain of study, but the rainfall intensity and duration are specified using different spatial patterns: (1) both $\bar{i}_r$ and $\bar{t}_r$ are kept spatially homogeneous and remain constant, (2) $\bar{i}_r$ increases with elevation, mimicking conditions in upwind slopes, and (3) $\bar{i}_r$ decreases with elevation, mimicking conditions in leeward slopes, as shown in equations (19a)–(19c) respectively:

$$\begin{cases} \bar{i}_r = 10 \text{ mm/hr} \\ \bar{t}_r = 1 \text{ hr} \end{cases} \tag{19a}$$

$$\begin{cases} \bar{i}_r = (10 + 2z) \text{ mm/hr} \\ \bar{i}_r * \bar{t}_r = 10 \text{ mm} \end{cases} \tag{19b}$$

$$\begin{cases} \bar{i}_r = (10 - 2z) \text{ mm/hr} \\ \bar{i}_r * \bar{t}_r = 10 \text{ mm} \end{cases} \tag{19c}$$

where z is the elevation in km.

[32] The results for precipitation patterns with different spatial behaviors are compared against the condition that both $\bar{i}_r$ and $\bar{t}_r$are kept spatially homogeneous in Figure 6. Figure 6 shows that even if the total precipitation ($\bar{i}_r$* $\bar{t}_r$) is kept spatially homogeneous, there are appreciable differences for channel profiles and gradients between cases with different spatial behaviors of $\bar{i}_r$ and $\bar{t}_r$. If $\bar{i}_r$ decreases with elevation and $\bar{t}_r$ increases at the same time as shown equation (19c), both the channel head elevation and the channel gradient tend to be greater than that with constant $\bar{i}_r$ and $\bar{t}_r$. This result implies that the effects of reduced erosion due to decreasing rainfall intensity with elevation cannot be

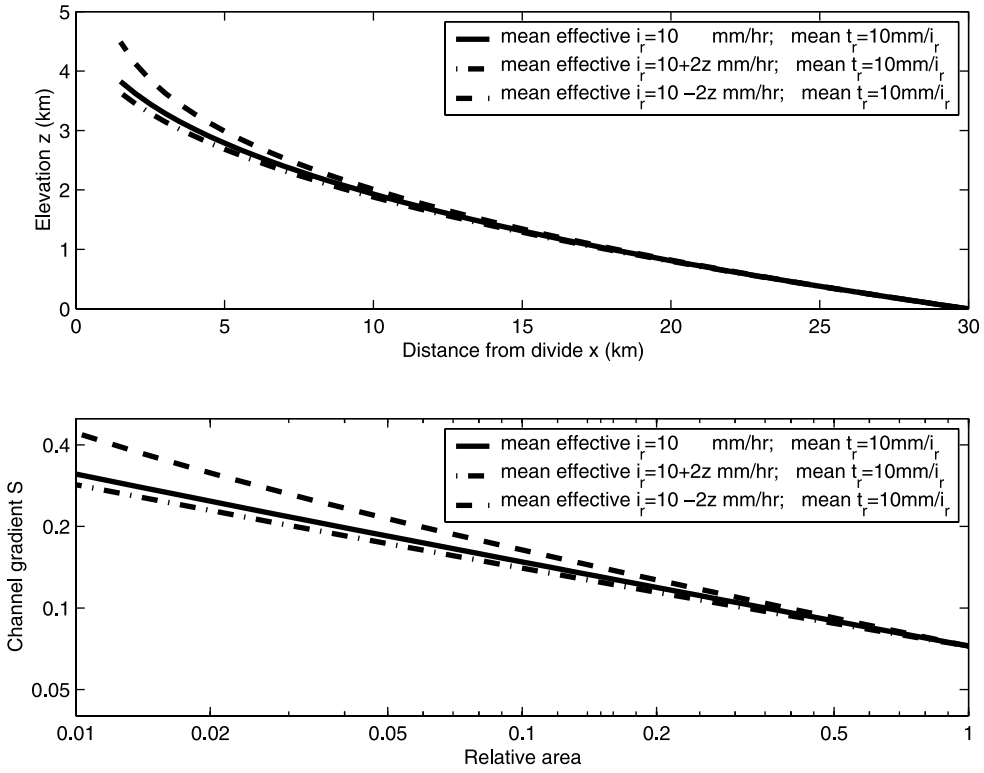

Figure 6. Effects of orographic precipitation on (top) channel profile and (bottom) slope.

counterbalanced completely by the contrarian effects from concurrent increases in rainfall duration, provided that the total precipitation amount remains constant. In contrast, if $\bar{i}_r$ increases with elevation and $\bar{t}_r$ decreases at the same time as shown equation (19b), both the channel head elevation and the channel gradient tend to be lower.

4. Conclusions and Discussion

[33] Precipitation has a strong effect on landscape evolution and whenever there is significant variation of total precipitation, there will always be significant influence on the evolution of channel profile. The general expectation is that higher annual precipitation would result in flatter channel profiles and lower channel heads. These results are consistent with previous studies [e.g., *Roe et al.*, 2003]. However, our results also demonstrate that the channel profile is not only sensitive to the total precipitation, but also to the detailed precipitation properties including the rainfall frequency, intensity, duration; and the distribution of these properties in space. The choice of probabilistic models for the intensity and duration of precipitation is also important. The channel profile is most sensitive to the variation of rainfall intensity and less sensitive to rainfall frequency and duration. This implies that, even for the same amount of precipitation, changes in rainfall regimes may have potentially significant impacts on landform and landscape evolution. Shorter and more intense rainfall could lead to significantly higher erosion rate and flatter channel profiles compared to longer and less intense rainfall. The reason for this is that rainfall intensity and duration have different implications on rainfall-runoff response and consequently the peak discharge and erosion rate. The spatial variation of precipitation can also influence the evolution of channel profile. Even if the total precipitation remains spatially homogeneous, different spatial behavior of rainfall intensity and rainfall duration may lead to different steady state profiles for river channel. The channel profile tends to be flatter under the conditions of increasing rainfall intensity and decreasing rainfall duration with elevation and vice versa.

[34] These results suggest that the application of the stream power law for erosion studies in mountainous regions should be conducted in the context of regional climate as described by the statistical properties of rainfall. They also have implications for our understanding of the effects of precipitation on landscape evolution, especially when there are significant variations of precipitation properties involved. For example, studies of the impact on long-term climate change on the landscape cannot be solely based on changes to total rainfall amounts. The storm properties and their distribution in space are important. This work provides insight to a fundamental question in landscape evolution, and that is whether it should be viewed in the context of response to discrete heavy precipitation events or in terms of uniform average rates over long periods of time [*Montgomery and Brandon*, 2002; *Barros et al.*, 2006].

[35] One issue we do not discuss in this paper but might be of considerable interest is the consideration of an erosion threshold in the stream power erosion law. *Tucker and Bras* [2000] and *Tucker* [2004] found that the presence of a threshold value for erosion can influence the predicted sensitivity of landscape evolution to rainfall variability. They pointed out that erosion rates will increase with the

increase of rainfall variability when a threshold value for erosion is incorporated, but without the presence of the threshold value, greater erosion is expected with less variable discharge for the case of $m < 1$). Variability in their case was defined only in terms of the ratio of the mean storm intensity to the mean annual rainfall. This is appropriate in their case since discharge was assumed to be a function of area, and hence only of storm intensity over the area. The magnitude of their discharge did not depend on storm duration. Our results, however, suggest that even without incorporating the erosion threshold, the predicted erosion rate would increase with higher mean precipitation intensity. There is no reason to believe that the addition of a threshold will change this. Answering why our intuitive result differs from their is not simple, but clearly it has to do with the approximations made. In this work, the discharge varies with time and depends on both rainfall intensity and duration. Equally important, it depends on the slope of the basin. The solution for the equilibrium profile is highly nonlinear because of the feedbacks between the topography and the hydrology. That is not the case in the work of *Tucker and Bras* [2000]. Variability in our context is not simply measured in terms of the ''peakiness'' of storms but of the combined variability of the distributions of mean rainfall intensity and duration.

[36] Some other factors including the erosion coefficient K, discharge exponent m and area exponent n in the stream power erosion model as well as the base level lowering rate U can influence the simulation results, including the magnitude of channel profile's sensitivity to precipitation properties. Nevertheless, given the clear first-order relationship between the profiles and the corresponding mean peak discharge shown in Figures 5a and 5b we are confident that changes in the above parameters will not diminish the sensitivity of channel profile to precipitation properties, nor influence the relative importance of rainfall intensity and duration in controlling the evolution of channel profile.

[37] **Acknowledgments.** This work started while R. L. Bras was enjoying a sabbatical at the Division of Engineering and Applied Sciences of Harvard University. R. L. Bras is grateful for the generosity of the Division and his host Ana Barros. Support has also been provided to R. L. Bras by the Army Research Office and CNR, Italy, through a collaborative agreement with MIT. This research was supported in part by NSF under grant EAR 9909647 with Ana Barros. We are also grateful to Gregory Tucker and Robert Anderson for very helpful comments.

References

Bacchi, B., G. Becciu, and N. T. Kottegoda (1994), Bivariate exponential model applied to intensities and durations of extreme rainfall, *J. Hydrol.*, *155*, 225–236.

Barros, A. P., and D. P. Lettenmaier (1994), Dynamic modeling of orographically induced precipitation, *Rev. Geophys.*, *32*, 265–284.

Barros, A. P., M. Joshi, J. Putkonen, and D. W. Burbank (2000), A study of the 1999 monsoon rainfall in a mountainous region in central Nepal using TRMM products and rain gauge observations, *Geophys. Res. Lett.*, *27*, 3683–3686.

Barros, A. P., G. Kim, E. Williams, and S. W. Nesbitt (2004), Probing orographic controls in the Himalayas during the monsoon using satellite imagery, *Nat. Hazards Earth Syst. Sci.*, *4*, 1–23.

Barros, A. P., S. Chiao, T. J. Lang, J. Putkonen, and D. Burbank (2006), From weather to climate—Seasonal and interannual variability of storms in the Himalayas, in *Tectonics, Climate and Landscape Evolution*, *Spec. Pap. Geol. Soc. Am.*, *398*, 17–38, doi:10.1130/2006.2398(02).

Bras, R. B. (1990), *Hydrology: An Introduction to Hydrologic Science*, 598 pp., Addison-Wesley, Boston, Mass.

Burbank, D. W., J. Leland, E. J. Fielding, R. S. Anderson, N. Brozovic, M. R. Reid, and C. C. Duncan (1996), Bedrock incision, rock uplift and threshold hillslopes in the northwestern Himalalyas, *Nature*, *379*, 505–510.

Flint, J. J. (1974), Stream gradient as a function of order, magnitude, and discharge, *Water Resour. Res.*, *10*, 969–973.

Goel, N. K., R. S. Kurothe, B. S. Mathur, and R. M. Vogel (2000), A derived flood frequency distribution for correlated rainfall intensity and duration, *J. Hydrol.*, *228*, 56–67.

Hancock, G. S., R. S. Anderson, and K. X. Whipple (1998), Bedrock erosion by streams: Beyond stream power, in *Rivers Over Rock: Fluvial Processes in Bedrock Channels*, *Geophys. Monogr. Ser.*, vol. 107, edited by K. Tinkler and E. Wohl, pp. 35–60, AGU, Washington, D. C.

Henderson, F. M. (1963), Some properties of the unit hydrograph, *J. Geophys. Res.*, *68*, 4785–4793.

Howard, A. D., and G. Kerby (1983), Channel changes in badland, *Geol. Soc. Am. Bull.*, *94*, 739–752.

Howard, A. D., W. E. Dietrich, and M. A. Seidl (1994), Modeling fluvial erosion on regional to continental scales, *J. Geophys. Res.*, *99*, 13,971–13,986.

Lave, J., and J. P. Avouac (2001), Fluvial incision and tectonic uplift across the Himalayas of central Nepal, *J. Geophys. Res.*, *106*, 26,561–26,592.

Leopold, L. B., and T. Maddock Jr. (1953), The hydraulic geometry of stream channels and some physiographic implications, *U. S. Geol. Surv. Prof. Pap.*, *252*.

Masek, J. G., B. L. Isacks, T. L. Gubbels, and E. J. Fielding (1994), Erosion and tectonics at the margins of continental plateaus, *J. Geophys. Res.*, *99*, 13,941–13,956.

Moglen, G. E., and R. L. Bras (1995), The effect of spatial heterogeneities on geomorphic expression in a model of basin evolution, *Water Resour. Res.*, *31*, 2613–2623.

Molnar, P. (2001), Climate change, flooding in arid environments, and erosion rates, *Geology*, *29*, 1071–1074.

Montgomery, D. R. (1994), Valley incision and the uplift of mountain peaks, *J. Geophys. Res.*, *99*, 13,913–13,921.

Montgomery, D. R., and M. T. Brandon (2002), Topographic controls on erosion rates in tectonically active mountain ranges, *Earth Planet. Sci. Lett.*, *201*, 481–489.

Montgomery, D. R., and W. E. Dietrich (1992), Channel initiation and the problem of landscape scale, *Science*, *255*, 826–830.

Rodriguez-Iturbe, I., and J. B. Valdes (1979), The geomorphologic structure of hydrologic response, *Water Resour. Res.*, *15*, 1409–1420.

Rodriguez-Iturbe, I., M. Gonzalez-Sanabria, and R. L. Bras (1982), A geomorphoclimatic theory of the instantaneous unit hydrograph, *Water Resour. Res.*, *18*, 877–886.

Roe, G. H., D. R. Montgomery, and B. Hallet (2002), Effects of orographic precipitation variations on the concavity of steady-state river profiles, *Geology*, *30*, 143–146.

Roe, G. H., D. R. Montgomery, and B. Hallet (2003), Orographic precipitation and the relief of mountain ranges, *J. Geophys. Res.*, *108*(B6), 2315, doi:10.1029/2001JB001521.

Rosenbloom, N. A., and R. S. Anderson (1994), Evolution of the marine terraced landscape, Santa Cruz, California, *J. Geophys. Res.*, *99*, 14,013–14,030.

Seidl, M. A., and W. E. Dietrich (1992), The problem of channel erosion into bedrock, *Catena Suppl.*, *23*, 101–124.

Seidl, M. A., W. E. Dietrich, and J. W. Kirchner (1994), Longitudinal profile development into bedrock: An analysis of Hawaiian channels, *J. Geol.*, *102*, 457–474.

Sklar, L., and W. E. Dietrich (1998), River longitudinal profiles and bedrock incision models: Stream power and the influence of sediment supply, in *Rivers Over Rock: Fluvial Processes in Bedrock Channels*, *Geophys. Monogr. Ser.*, vol. 107, edited by K. J. Tinkler and E. E. Wohl, pp. 237–260, AGU, Washington, D. C.

Snyder, N. P., K. X. Whipple, G. E. Tucker, and D. J. Merritts (2000), Landscape response to tectonic forcing: digital elevation model analysis of stream profiles in the Mendocino triple junction region, northern California, *Geol. Soc. Am. Bull.*, *112*, 1250–1263.

Snyder, N. P., K. X. Whipple, G. E. Tucker, and D. J. Merritts (2002), Interactions between onshore bedrock-channel incision and near-shore wave base erosion forced by eustasy and tectonics, *Basin Res.*, *14*, 105–127.

Solyom, P. B., and G. E. Tucker (2004), Effect of limited storm duration on landscape evolution, drainage basin geometry, and hydrograph shapes, *J. Geophys. Res.*, *109*, F03012, doi:10.1029/2003JF000032.

Stock, J. D., and D. R. Montgomery (1999), Geologic constraints on bedrock river incision using the stream power law, *J. Geophys. Res.*, *104*, 4983–4993.

Tucker, G. E. (2004), Drainage basin sensitivity to tectonic and climatic forcing: Implications of a stochastic model for the role of entrainment and erosion thresholds, *Earth Surf. Processes Landforms*, *29*, 185–205.

Tucker, G. E., and R. L. Bras (1998), Hillslope processes, drainage density, and landscape morphology, *Water Resour. Res.*, *34*, 2751–2764.

Tucker, G. E., and R. L. Bras (2000), A stochastic approach to modeling the role of rainfall variability in drainage basin evolution, *Water Resour. Res.*, *36*, 1953–1964.

Tucker, G. E., and K. X. Whipple (2002), Topographic outcomes predicted by stream erosion models: Sensitivity analysis and intermodel comparison, *J. Geophys. Res.*, *107*(B9), 2179, doi:10.1029/2001JB000162.

Whipple, K. X. (2004), Bedrock rivers and the geomorphology of active orogens, *Annu. Rev. Earth Planet. Sci.*, *32*, 151–185.

Whipple, K. X., and G. E. Tucker (1999), Dynamics of the stream-power river incision model: Implications for height limits of mountain ranges, landscape response timescales and research needs, *J. Geophys. Res.*, *104*, 17,661–17,674.

Whipple, K. X., and G. E. Tucker (2002), Implications of sediment-flux-dependent river incision models for landscape evolution, *J. Geophys. Res.*, *107*(B2), 2039, doi:10.1029/2000JB000044.

Whipple, K. X., E. Kirby, and S. H. Brocklehurst (1999), Geomorphic limits to climate-induced increases in topographic relief, *Nature*, *401*, 39–43.

Whipple, K. X., G. S. Hancock, and R. S. Anderson (2000a), River incision into bedrock: Mechanics and the relative efficacy of plucking, abrasion, and cavitation, *Geol. Soc. Am. Bull.*, *112*(3), 490–503.

Whipple, K. X., N. P. Snyder, and K. Dollenmayer (2000b), Rates and processes of bedrock incision by the Upper Ukak River since the 1912 Novarupta ash flow in the Valley of Ten Thousand Smokes, Alaska, *Geology*, *28*, 835–838.

Willgoose, G., and R. L. Bras (1991), A coupled channel network growth and hillslope evolution model: 1. Theory, *Water Resour. Res.*, *27*, 1671–1684.

Wolman, M. G., and J. P. Miller (1960), Magnitude and frequency of forces in geomorphic processes, *J. Geol.*, *68*, 54–74.

A. P. Barros, Department of Civil and Environmental Engineering, Duke University, Durham, NC 27708, USA.

R. L. Bras, Department of Civil and Environmental Engineering, Massachusetts Institute of Technology, Cambridge, MA 02139, USA.

S. Wu, Division of Engineering and Applied Sciences, Harvard University, 29 Oxford Street, Cambridge, MA 02138, USA. (wu18@fas.harvard.edu)